Cell. Mol. Life Sci. 65 (2008) 1378 – 1389
1420-682X/08/091378-12
DOI 10.1007/s00018-008-7507-6

Cellular and Molecular Life Sciences

Review

Myosin V from head to tail

K. M. Trybus

Department of Molecular Physiology and Biophysics, 149 Beaumont Avenue, University of Vermont, Burlington, Vermont 05405 (USA), Fax: +1-802-656-0747, e-mail: kathleen.trybus@uvm.edu

Received 31 October 2007; received after revision 4 December 2007; accepted 2 January 2008
Online First 1 February 2008

Abstract. Myosin V (myoV), a processive cargo transporter, has arguably been the most well-studied unconventional myosin of the past decade. Considerable structural information is available for the motor domain, the IQ motifs with bound calmodulin or light chains, and the cargo-binding globular tail, all of which have been crystallized. The repertoire of adapter proteins that link myoV to a particular cargo is becoming better understood, enabling cellular transport processes to be dissected. MyoV is processive, meaning that it takes many steps on actin filaments without dissociating. Its extended lever arm results in long 36-nm steps, making it ideal for single molecule studies of processive movement. In addition, electron microscopy revealed the structure of the inactive, folded conformation of myoV when it is not transporting cargo. This review provides a background on myoV, and highlights recent discoveries that show why myoV will continue to be an active focus of investigation.

Keywords. Myosin V, motor protein, IQ motif, cargo-binding, processivity, calmodulin.

Biological role

MyoV provides continuous transport of organelles, membranous cargo, secretory vesicles, mRNA, lipids and proteins vesicles on actin tracks [1], while kinesin and dynein provide comparable services on microtubule tracks. Class V myosins are found in organisms as primitive as yeast, which contain two class V myosins. In humans, there are three class V myosins (Va, Vb, and Vc), each with different tissue specificities, that are associated with a specific set of membrane trafficking events [2]. MyoVa is primarily expressed in brain and melanocytes. Mice lacking myoVa have aberrant coat colors due to defects in melanosome trafficking, and die at several weeks due to neurological seizures [3]. Humans with defects in myoVa, or the proteins that act as adapters between myoVa and cargo, develop Griscelli syndrome, a disease characterized by pigmentation defects and neurological symptoms [4]. MyoVb and myoVc are primarily expressed in epithelial cells, and have been implicated as motors involved in recycling endosomes [2, 5, 6]. MyoV and its associated cargoes are thus key components of anterograde transport pathways that move and/or anchor cargo near the cell periphery.

Overview

MyoV can be divided into four major structural domains (Fig. 1A). The motor domain contains the actin-binding site and nucleotide-binding site, followed by an extended 24-nm α-helical lever arm that is stabilized by binding six calmodulins (CaMs), or related light chains. The lever arm amplifies small nucleotide-dependent changes that originate at the active site, allowing a large power stroke to occur following ATP hydrolysis. The rod region follows, which contains regions of α-helical coiled-coil that are responsible for dimerization of the molecule. At the C

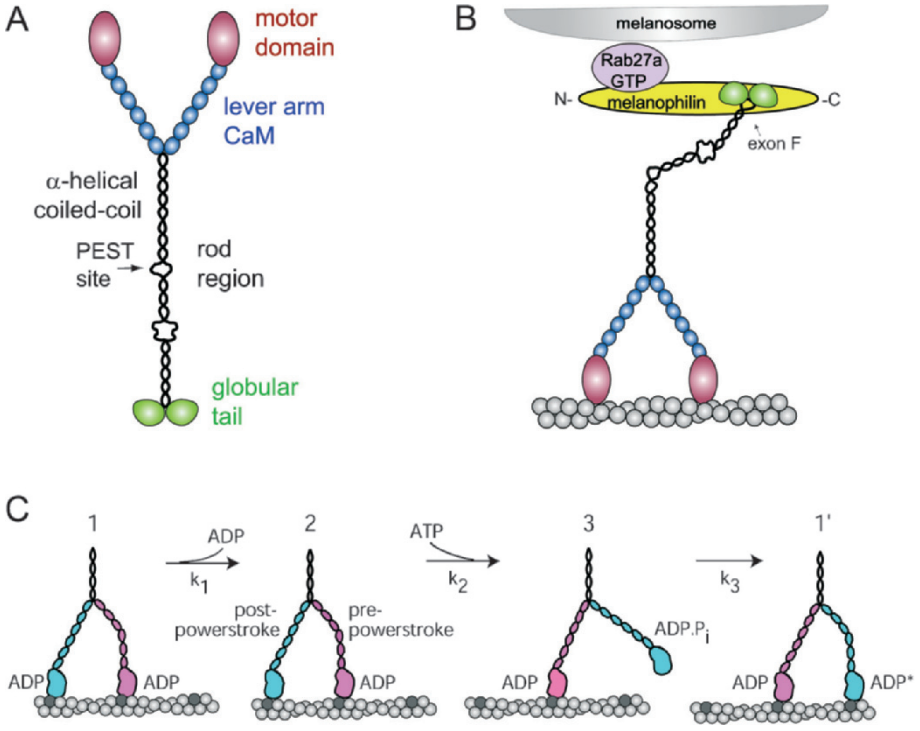

Figure 1. (*A*) Domain structure of myosin Va (myoVa). At the N terminus, the motor domain contains the actin-binding site and nucleotide-binding site, followed by an ~24-nm-long lever arm that binds six calmodulins (CaM) or related light chains. The rod region of myoVa contains three stretches of α-helical coiled-coil, which are interrupted by two major regions of non-coiled-coil. At the C terminus, the globular tail binds adapter proteins that link it to cargo. (*B*) The melanosome receptor complex for myoVa. Binding of myoV to the C-terminal region of melanophilin requires both the globular tail and the alternatively spliced exon F in the rod. Exon F is present in melanocyte but not in brain myoVa. Melanophilin connects myoVa to melanosomes *via* its interaction with Rab27a in the GTP-bound state. Figure adapted from [38]. (*C*) A general model for processive movement. Starting in state 1, both heads are strongly bound to actin with ADP at the active site. The trailing head is in a post-power stroke conformation, and the leading head is in a strained, pre-power stroke state. The trailing head releases ADP at ~12 s^{-1} (k_1), the rate limiting step of the ATPase cycle (state 2). ATP binds to the trailing head and dissociates it from actin, allowing the attached head to complete its power stroke. At the same time, the detached head is thrust forward, hydrolyzes ATP, and becomes the new leading head in a pre-power stroke conformation (state 3). The detached head undergoes a diffusive search for the next actin binding site, releases P_i, and undergoes a transition to the strong binding state. State 1' shows that the leading head may pass through an isomerized ADP* state before returning to state 1 [70]. The darker gray actin monomers are located ~36 nm apart to illustrate the size of each step. Figure adapted from [10].

terminus is a globular tail that binds adapter proteins that link myoV to cargo (Fig. 1B).

MyoV is a processive motor, using a hand-over-hand mechanism to move it forward in many 36-nm steps before dissociating from actin. In the two-head bound state, the trailing head is in a post-power stroke conformation, and the leading head is in a strained, pre-power stroke state (Fig. 1C). Long run lengths are achieved by coordinating the stepping of the two heads *via* intramolecular strain, so that the leading head does not dissociate prematurely. When the trailing head is dissociated by ATP, the bound head completes its power stroke. The detached head is thrust forward, re-primes its lever arm into a pre-power stroke state, and searches for the next actin-binding site. The motor/cargo complex thus moves forward on actin.

Motor domain

The overall structure of the myoV motor domain is similar to that of previously crystallized motors (Fig. 2A). Nonetheless, it revealed several novel features that show why tight binding to actin and tight binding to ATP are mutually exclusive. The first crystal structure of myoV was obtained in the absence of nucleotide [7, 8]. For the first time, the large internal cleft that separates the actin-binding interface was totally closed, due to Van der Waal's and specific side-chain interactions between residues on either side of the cleft (the so-called upper and lower 50-kDa domains). This closure brought together elements of the actin binding interface on either side of the cleft that are consistent with the expected high affinity of the nucleotide-free state for actin. The major structural rearrangement needed to obtain cleft closure was a large distortion of an internal seven-stranded β

sheet, and a large rotation of the upper 50-kDa domain. The seven-stranded β sheet, along with associated loops and linkers, has been coined the "transducer" (Fig. 2A, right panel). These domain movements restructured the nucleotide-binding elements (P-loop, switch 1, and switch 2) so that they can no longer strongly co-ordinate nucleotide. The complete cleft closure seen with nucleotide-free myoV even in the absence of actin might facilitate the transition to a strong binding state, which is an important feature for a processive motor. Conversely, crystals obtained with the ATP analog ADP.BeF_x showed that the nucleotide-binding elements have been repositioned to co-ordinate ATP, and in doing so the cleft is reopened, while the lever arm remains in a downward, post-power stroke position.

Electron cryomicroscopy of actin filaments decorated with myoV further provided models of the actin-bound myoV motor domain. Crystal structures are docked into the three-dimensional reconstructions to generate atomic models of acto-myoV [9]. The relatively high affinity of the myoV motor domain for actin in the so-called "weak-binding" states (with ATP or ADP.P_i at the active site) was exploited to obtain two new actin-bound states. In the presence of ATP, the long cleft dividing the actin-binding region of the motor domain opens and effectively destroys the strong-binding interface, while leaving the lever arm in a downward post-power stroke conformation. This and the crystal structures described above provide a structural mechanism to explain how ATP dissociates myosin from actin. The second new actin-bound state, obtained with nucleotide analogs (AMP-PNP or ADP.AlF_4), showed for the first time the lever arm in an upward, pre-power stroke conformation, that would be occupied prior to phosphate release [9].

The importance of loop 2 as a tether to help maintain contact with actin was also established. Loop 2 is a surface loop at the actin-binding interface that is involved in the initial weak electrostatic interaction of myosin with actin. It is disordered in the unbound crystal structures, but becomes ordered when myoV binds to actin [9]. Density for loop 2 on actin is reconfigured as the nucleotide state changes. Mutational studies showed that the net positive charge of loop 2 plays a role in determining processive run length. Decreasing the positive charge in loop 2 causes processive runs to terminate sooner than with wild-type myoV, while increasing the net positive charge of loop 2 enhances run lengths [10]. These observations suggest that a high affinity for actin while in the weak-binding state, mediated by loop 2, allows a detached head of a processively moving myoV to more readily find its next binding site and continue a processive run.

Lever arm

The lever arm of myoV contains six IQ motifs, each with consensus sequence IQxxxRGxxxR, where x denotes any amino acid. The number of amino acids between adjacent motifs alternates between 23 and 25, such that the lever arm can be described as three pairs of IQ motifs. Each motif binds CaM, or related light chains that have not retained functional calcium-binding sites. CaM has four high-affinity calcium-binding sites called EF-hands, each composed of two α-helices connected by a calcium-binding loop. Murine myosin Va isolated from tissue only binds CaM [11], while that isolated from chicken brain contains both CaM and a specific light chain of the essential light chain family (called L17 or L23) [12–14]. Based on analysis of proteolytic fragments of myoVa purified from chick brain, it was concluded that the specific light chain does not bind to IQ motif one or two [14]. In contrast, when expressed *in vitro*, the first IQ motif can bind either CaM or a specific light chain, showing that the specificity of an IQ motif for a particular subunit is not all-or-none. This result raises the question of whether the subunit that occupies a given IQ motif can vary *in vivo*, depending on expression levels of the relevant light chains.

Why does it matter whether CaM or a light chain binds to a particular motif? First, calcium can only effect regions of the lever arm to which CaM is bound. Second, kinetic analysis showed that the presence of the light chain adjacent to the motor domain alters rate constants such that the M.ADP.P_i state is favored, compared to when CaM is bound in this position [15]. A single-molecule study, in which one head of myoV was labeled with a gold nanoparticle, showed that rebinding of the free head during a processive run was threefold slower when CaM was exclusively bound to the lever arm, compared to when a light chain was also bound [16]. This might give the free head more time to find its next actin binding site and continue a processive run, which could be advantageous *in vivo*, given the complex nature of the intracellular milieu.

The crystal structures of several IQ motifs of Myo2p (a class V myosin from the budding yeast *Saccharomyces cerevisiae*), in complex with the light chain Mlc1p, have been determined. Unlike CaM, Mlc1p does not bind calcium. The structure of Mlc1p bound to single IQ motifs (two and four) [17], and to the two-three pair [18], allowed a model for the entire lever arm to be proposed. One conclusion was that there is little interaction between pairs of IQ motifs, implying that the regions between the second and third, or fourth and fifth IQ motifs, might provide a hinge region to allow the lever arm to bend into the telemark conformation observed in electron microscopic im-

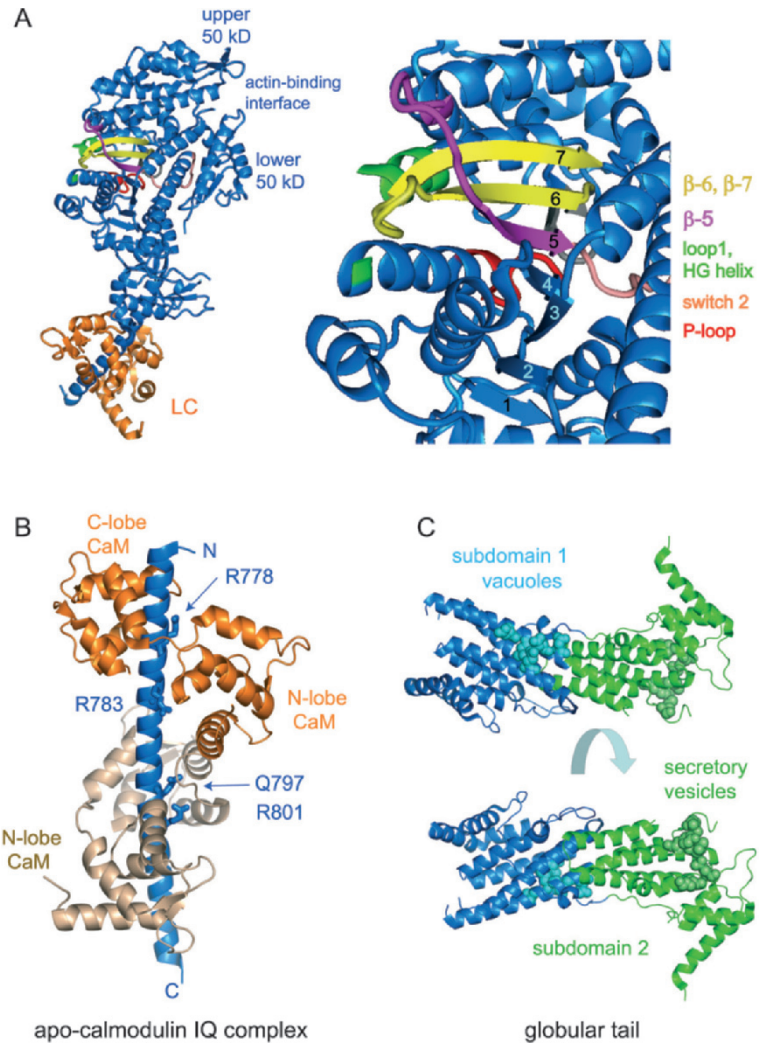

Figure 2 Crystal structures of domains of myoV. (*A*) Ribbon diagram of nucleotide-free myoV (PDB, 1oe9). (Left) Overview of the motor domain-light chain (LC) complex in the absence of nucleotide, which is the structural model for the strong-binding rigor state. (Right) An enlarged view of the transducer region, which is the central region of the motor domain near the active site. It includes the last three strands of the seven-stranded β sheet (magenta and yellow) and other regions that accommodate the distortion that occurs between the rigor and post-rigor states, including loop 1 (missing residues that connect the green ends), and the bulge between β strands six and seven. Closure of the actin-binding cleft unexpectedly distorted the central β sheet, and significantly modified the active site so that it cannot bind nucleotide. (*B*) Ribbon diagram of apo-CaM bound to the first two IQ motifs of murine myoV (PDB, 2ix7). The two IQ motifs are shown in blue ribbon. Some of the side chains of the consensus residues of the IQ motif (IQxxxRGxxxR) are shown in stick representation. For the first motif, which binds the orange-colored CaM, both consensus Arg residues are shown. The consensus Gln and the first Arg (position 6 of the motif) are shown for the second IQ motif. The consensus residues in each IQ motif do not show the same interaction with CaM. The two lobes of CaM are each composed of four helices. The four calcium binding sites, each of which is formed by a loop connecting a pair of α-helices, are not occupied in this structure. CaM can bind to the IQ motif in the absence of calcium because the C-lobe is in a semi-open, gripping conformation that binds the first half of the consensus sequence. The N-lobe is in a closed, non-gripping conformation that interacts more weakly with the second half of the IQ motif. This differs from unbound apo-CaM in which both the N-lobe and the C-lobe are closed. (*C*) Ribbon diagram of the globular tail of Myo2p, the class V myosin from budding yeast (PDB, 2f6 h). The overall structure consists of two five-helical bundles connected by varying sized loops. A long central helix (H6) connects the two subdomains, shown in blue (subdomain 1), and green (subdomain 2). The residues depicted in space-filling representation have been implicated in vacuole binding (cyan), or in secretory vesicle binding (light green). Note that the two binding sites are on opposite sides of the globular tail.

ages [19]. Subsequent molecular dynamics simulations of the IQ motifs suggested that the sequence of the fourth IQ motif may harbor a flexible joint that enables the elasticity of the myoV lever arm [20]. A second conclusion of the crystallographic studies was that the N-lobe of Mlc1p does not interact with IQ motifs 4 and 6, leaving it free to potentially interact with another binding partner. NMR studies further showed that MLC1p also binds to the first IQ motif of Myo2p only *via* its C-lobe, leaving the N-lobe free to bind another target [21]. In contrast, CaM binds to IQ1 with both lobes based on fluorescence resonance

energy transfer studies [18]. The different behavior of CaM and Mlc1p with respect to the first IQ motif of Myo2p appears to be related both to unique structural features of the N-lobe of Mlc1p, particularly the fifth D' helix that stabilizes a closed lobe structure, and to the exact sequence of the IQ motif [21]. These different modes of binding may explain why Mlc1p has an essential function for vesicle targeting that is not shared by CaM. In vertebrate myoV, it was also suggested that the lever arm might be involved in binding other proteins. MyoV on synaptic vesicles interacts with syntaxin-1A, a t-SNARE involved in exocytosis [22]. In the vertebrate case, syntaxin binds to an IQ motif from which CaM had dissociated, and not to a free lobe of a light chain as proposed for yeast myoV.

Unconventional myosins are unusual in that CaM binds the most strongly to the IQ motifs in the absence of calcium. How is this accomplished, given that CaM typically binds to its target peptides only in the presence of calcium? Calcium causes the two lobes of CaM to adopt an open, gripping conformation that binds targets that contain a basic amphiphilic helix. The two lobes of apo-CaM, in contrast, adopt a closed, non-gripping conformation [23, 24]. The crystal structure of CaM bound to the first two IQ motifs of mouse myoV resolved this paradox. The structure showed that the C-terminal lobe of apo-CaM adopts a semi-open conformation that grips the first part of the IQ consensus sequence (IQxxxR), while the closed N-terminal lobe interacts more weakly with the second half of the consensus sequence (GxxxR) [25] (Fig. 2B). A surprising finding was that the non-consensus residues of the motif play a key role in the exact positioning of the two lobes of CaM, resulting in the consensus residues of each motif interacting differently with CaM along the length of the lever arm. Calcium has two effects on CaM bound to an IQ motif in the lever arm. Low micromolar calcium concentrations unfold and activate the inhibited state of myoV (discussed in a subsequent section). Higher calcium concentrations act as a "brake". *In vitro* motility ceases [26], and processive runs of single myoV molecules are terminated [27]. The basis for the inhibition is dissociation of a bound CaM, rendering the lever arm compliant and unable to communicate strain-dependent information between the heads. Several lines of evidence suggest that CaM dissociates from IQ motif 2 at high calcium concentration [14, 28]. Electron cryomicroscopy also showed that calcium causes a major rearrangement of the bound CaM [28]. The extent to which calcium affects function *in vivo* is not known.

Another role of the long lever arm is to allow myoV to take 36-nm steps along actin, which is equal to the pseudo repeat of the actin helix. It is well-established that the step size of monomeric myoV constructs containing one to six IQ motifs increases with lever arm length [29–31]. In double-headed constructs, it was also shown that the step size of myoV is determined by neck length and not by the pseudo-repeat of the actin filament [31]. The 25-nm working stroke of a monomer containing the complete lever arm with six IQ motifs is, however, smaller than the 36-nm step taken by a six-IQ double-headed motor walking processively. This implies that the 36-nm step of the native molecule is a combination of the working stroke (25 nm) of the bound head and a biased, thermally driven diffusive movement (11 nm) of the free head onto the next actin-binding site [32]. Further evidence in favor of myoV actively moving cargo *via* a lever arm mechanism was obtained in a study in living yeast. Mutants of Myo2p (a yeast class V myosin) with varying lever arm lengths caused secretory vesicles to move toward their site of exocytosis with speeds that correlated with the lever arm length [33]. This active movement of cargo by myoV in budding yeast is in contrast to passive capture and tethering mechanisms suggested for myoV in melanocytes, where microtubule-based motors are the primary long-distance active motors [34, 35].

Rod region

The rod region lies between the IQ motifs and the globular tail, and contains varying amounts of sequence with a propensity to form α-helical coiled-coil. In myoVa, there are three major regions of coiled-coil, with two interruptions (Fig. 1A). The propensity to form α-helical coiled-coil is based on the strength of the heptad repeat, a seven amino acid motif in which the first and fourth positions, which form the internal seam of the coiled-coil, are hydrophobic amino acids. The rod of myoVa has a total of ~60 heptad repeats of coiled-coil, and the first ~20 heptad repeats before the PEST site are sufficient to ensure dimerization. Dimeric constructs truncated just before the PEST site are referred to as myoV-HMM (heavy meromyosin, by analogy with proteolytic subfragments of conventional class II myosin). The first interruption in the coiled-coil is a PEST site, which contains amino acids Pro(P), Glu(E), Ser(S), and Thr(T). This region can be cleaved *in vitro* by the protease calpain [36], although its role *in vivo* is not known. PEST sites are generally thought to decrease the half-lives of proteins that contain them. The advantage of rapid turnover for myoV is unclear, unless the process can be regulated. MyoVc lacks this PEST site [2].

Two other major regions of coiled-coil follow the PEST site in myoVa (one with ~12 heptads, the other

with ~20 heptads), interrupted by a break of ~80 amino acids. The region of the tail after the PEST site contains exons A–F, three of which (B, D, and F) are alternatively spliced in different tissues, giving rise to multiple isoforms. Some, but not all, of these exons contain heptad repeats. An isoform prevalent in brain contains exons A, B, C, and E, while that in melanocytes contains A, C, D, E, and F [37]. Exon F is essential for interaction with melanosomes [38]. This was the first example showing that alternative exon usage in the rod can help specify particular cargoes, in addition to binding sites for cargo in the globular tail. The brain-specific exon B contains only three amino acids (DDK), but is essential for binding an ~10-kDa light chain in the dynein family called DYNLL2 [39, 40], which co-purifies with myoVa isolated from chick brain [13]. Spectroscopic studies showed that binding of DYNLL2 increases the α-helical coiled-coil content in the region around its binding site. In addition, it has been proposed that DYNLL2 acts as an adapter between myoVa and various cargoes such as the pro-apoptotic protein Bmf [41] and the postsynaptic scaffolding protein GKAP (guanylate kinase domain-associated protein) [42].

Globular tail domain

The C-terminal ~400 amino acids of myoV comprise a globular tail domain that has two known roles: cargo binding *via* cargo-specific receptors, and stabilization of the folded, inhibited conformation of myoV *via* an interaction with the motor domain. The globular tail of Myo2p (a yeast class V myosin) consists of two functional domains that specify vacuole-specific or secretory vesicle-specific cargo [43]. Mutational studies identified amino acids that affected only one or the other of these processes [44]. These observations were given a structural basis once the globular tail domain was crystallized (Fig. 2C) [45]. The tail consists of two five-helical bundles connected by a common long helix. Point mutations that disrupt Vac17p binding cluster along a solvent-exposed face of helix 6. The binding site for secretory vesicles, the essential cargo of Myo2p, was mapped to a distinct location in subdomain 2, which did not overlap with the vacuole-binding region. The two sites are at opposite ends of the globular tail and offset by approximately 180°. Both of these regions are highly conserved, implying that they may also bind organelle-specific receptors in myoV from higher organisms. Additional conserved patches of residues are distributed on the surface and may define other receptor-binding sites.

Adapter proteins that connect myosin V to cargo

Melanosomes are the most well-studied cargo of mammalian myoVa. Mutations in mice with lightened coat color identified three proteins as essential for successful movement of melanosomes. The *dilute* phenotype arises from mutations in the globular tail or motor domain of myoV [46], the *leaden* phenotype from mutations in melanophilin (also called Slac2-a) [47], and the *ashen* phenotype arises from defects in Rab27a, a small GTPase of the Ras superfamily [48]. These three proteins constitute an organelle-specific transport complex (Fig. 1B). Rab27a localizes to the melanosome membrane, and in its GTP-bound form, recruits melanophilin to it, which binds to the myoVa tail in an exon F-dependent fashion [38, 49, 50]. The requirement for the GTP-bound form of the Rab provides a regulatory checkpoint for formation/dissolution of the cargo complex. Melanophilin has an N-terminal Rab27a effector domain, and a C-terminal myoV binding region (globular tail and exon F). The involvement of alternatively spliced exons in cargo binding allows a mechanism to select more alternative cargoes than would be possible if the globular tail alone were involved. The globular tail of myoVa binds to an intrinsically unstructured domain of melanophilin [51]. Why such a region would be utilized for binding is not clear, but one possibility is that it provides a site for rapid degradation following cargo delivery, in addition to the PEST site that melanophilin contains. MyoVa, melanophilin, and a dominant active GFP-tagged Rab27a have been reconstituted *in vitro* and shown to form a transport complex that moves processively on actin [52].

The generality of a cargo complex was shown with myoVb, where an Rab-binding protein called FIP2 acts as an adapter between myosin and Rab11a, a GTPase that binds to recycling endosomes, the cargo of myoVb [53, 54]. Rab8a has been recently implicated in non-clathrin-dependent endocytosis and recycling by myoVb [55]. Another well-characterized complex is the vacuole-specific receptor complex for Myo2p (yeast class V myosin), which consists of a vacuolar membrane-bound protein Vac8p, and an adapter protein Vac17p that links Vac8p to myosin. Neither Vac protein is an Rab. Either additional binding partners have yet to be identified, or this complex differs from the mammalian version. The linkage between Myo4p (another yeast class V myosin) and its cargo is also well-established. Myo4p transports over 20 different mRNAs and cortical endoplasmic reticulum to the yeast bud on actin cables. She3p acts as an adaptor between Myo4p and She2p, which binds the mRNA cargo (reviewed in [56]).

Cargo selection and delivery

Mammalian and yeast myoVs have multiple cargoes. The presence of multiple receptor-binding sites on the globular tail raises the question of how a particular cargo is selected. One possibility is that a particular organelle-specific receptor is expressed only when needed in the cell-cycle to prevent competition between cargoes. In budding yeast, the protein level of Vac17p changes with the cell cycle, and is likely to be the trigger that controls the start of vacuole movement [57]. Alternatively, the globular tail might undergo a conformational change to expose only one site at a time. Such a mechanism was proposed for the globular tail of a plant myosin XI, where it was suggested that the two domains of the globular tail alternate between different conformations in solution, and that organelle binding selects and stabilizes a particular conformation [58]. Binding of one cargo may then sterically preclude binding of another. Phosphorylation by calcium/calmodulin-dependent protein kinase II has also been shown to regulate cargo attachment in *Xenopus* oocytes in a cell-cycle dependent fashion, with phosphorylation resulting in detachment of cargo from the motor [59]. The generality of phosphorylation as a regulatory mechanism has not been established.

How does cargo know where to be delivered? One strategy is *via* regulated degradation of the transport complex once it arrives at the proper location. For the vacuole complex consisting of Myo2p/Vac17p/Vac8p in budding yeast, once the vacuole is properly deposited near the center of the bud, Vac17p is degraded *via* a PEST-dependent sequence [57]. Deletion of the PEST sequence within Vac17p causes a backward movement of the vacuoles, causing them to mislocalize to the neck between the mother cell and the bud. Melanophilin also contains a PEST site, a sequence that can specify rapid protein turnover [60]. A mutant melanophilin lacking the PEST site did not properly localize melanosomes in melanocytes, suggesting that degradation may be a necessary element for localization. Regulated disruption of the transport complex may be a general mechanism to deposit organelles at their proper destination. The final destination may also be specified by binding to an anchor protein that is located there.

Processivity: The active motor

MyoV was the first myosin identified as processive, meaning that it takes multiple steps on its track without dissociating [61]. Although many detailed models have been proposed to explain the processive movement of myoV (reviewed in [62]), a minimal model that describes the essential features is shown in Fig. 1C. Arbitrarily starting with both heads in an ADP-bound state, the trailing head releases ADP at approximately 12 s^{-1}, the rate limiting step in the cycle [63]. ATP binds and dissociates the trailing head, allowing the constrained leading head to complete its power stroke and release stored elastic energy. The detached head hydrolyzes ATP, reprimes its lever arm to a pre-power stroke position, and binds to the next actin binding site as the new leading head. Phosphate release is fast [63], and the molecule is back to the starting position with ADP bound to each head. Branched or alternate kinetic pathways during processive movement have also been suggested, which differ in the order that the leading and trailing heads adopt different nucleotide states [64, 65].

Several features optimize myoV for processivity. One head must remain bound to the actin filament at all times. The motor domain must therefore have a high duty cycle, meaning that it spends most of its time attached to actin in a strong binding state. This occurs because the rate-limiting step in the ATPase cycle is release of MgADP from an actin-bound head, at a rate of ~12 s^{-1} [63]. A second feature is a high affinity for actin in the weak-binding states (ATP or ADP.P_i at the active site) [66, 67], which likely enhances the ability of the new leading head to find its next binding site, as suggested by mutational studies [10, 68]. Third, strain-dependent changes in the kinetics of the two heads are accomplished through the long lever arms that join the two motor domains. This feature co-ordinates the two heads so that their kinetic cycles are out of phase. Intramolecular strain can accelerate the rate of ADP release from the rear head, inhibit the rate of ADP release from the lead head, or a combination of the two. The key feature is to prevent the leading head from dissociating prematurely. The rate of ADP release from the leading head appears to be the most affected, although this is still debated [69–72]. It is clear that strain-dependent kinetics are necessary to enhance processive run length [32].

Single-molecule approaches established that the mechanism of forward motion is hand-over-hand, meaning that the trailing and leading heads exchange position with every step [73, 74], Less is known about the intermediate that occurs as the rear head releases from actin in order to become the new trailing head. Gold nanoparticles attached to the lever arm allowed the motion of the free head to be tracked with submillisecond resolution [16]. The results showed that the unbound head can rotate freely about the lever-arm junction, in its search for the next actin-binding site. In an alternative approach, the motions of a stiff rod (a fluorescent microtubule) attached to

the lever arm were monitored to show that the free head undergoes Brownian motion in all directions before becoming the new leading head [75]. Ninety-degree rotations related to the detachment and rebinding of the heads to actin are also thought to occur by thermal twisting of the neck during a 36-nm step [76]. These features are likely to facilitate the movement of myoV through the crowded actin meshwork in the cell cortex by maximizing the possibility that the new leading head finds its next actin-binding site.

To what extent can individual steps of myoV be resolved *in vivo?* By tracking the cargo melanosome in *Xenopus* melanocytes with 2-nm accuracy, steps with a distribution around 35-nm were observed, the same as that observed *in vitro* [77]. The velocity was slower than expected based on *in vitro* studies, but subsequent experiments suggested that intermediate filaments may be responsible for hindering myoV transport by increasing viscous drag [78]. This latter study also showed some limited data on track switching *in vivo*, which opens the door for further studies on this important process.

Folded myosin V: The inhibited state

A critical feature of any motor is how its activity is turned off when it is not actively moving cargo. Hydrodynamic data provided the first evidence that myoV undergoes a change in conformation as it goes from an active to an inhibited state [26, 79, 80]. The active, extended state sedimented at ~11S, while the inhibited, folded conformation sedimented at ~14S. Intramolecular folding appears to be a common mechanism to inhibit the activity of motor proteins, as a similar conformational transition was shown previously with smooth muscle myosin [81, 82] and kinesin [83].

The three-dimensional structure of the folded monomer was determined by two complementary electron microscopic approaches. Two-dimensional arrays of myoV on lipid monolayers showed a repeating motif that resembled a six-petaled flower, each consisting of a folded monomeric myoV [84] (Fig. 3). An atomic model of the structure, built with available crystal structures, showed that myoV bends at the junction between the lever arm and the rod, so that the motor domain interacts with the globular tail, similar to a person touching his toes. The globular tail interacts with the motor domain near loop 1 at the entrance to the active site, which is far from the actin-binding site, suggesting that product release may be directly inhibited. A dominant feature of the structure was the extended lever arms, each with six bound CaMs. Both lever arms are in a post-power stroke orientation, suggesting that the folded molecule has the potential to bind strongly to actin. The coiled-coil region is skewed more toward one lever arm than the other. Approximately 21 nm of the coiled-coil, similar to the length of the rod before the PEST site, were visualized. The "missing" coiled-coil is likely disordered structure that constitutes the pistil of the flower motif. Consistent with this idea, a mutational study concluded that the globular tail binds to the C-terminal end of the coiled-coil just before the PEST site to stabilize the motor domain-globular tail interaction, creating the triangular appearance typical of the folded monomer [85]. To accomplish this, the remaining rod region between the PEST site and the globular tail would have to fold at the break between the remaining two regions of coiled-coil, which could account for the density in the center of the flower motif.

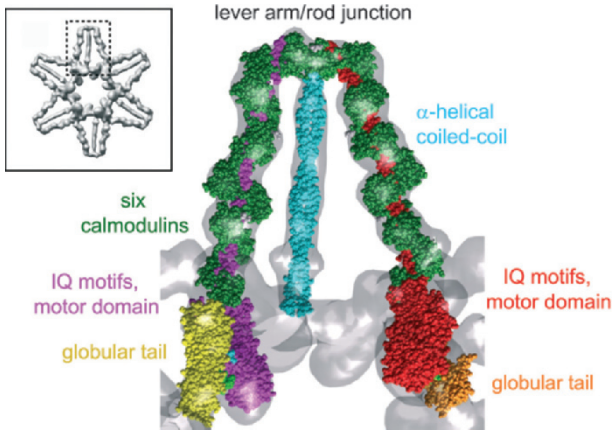

Figure 3. Three-dimensional structure of myoV in the folded, inactive conformation. The inset shows the overall flower-motif formed by two-dimensional arrays of myoV [84]. Each petal of the motif (dashed box) indicates one folded monomer. The larger view has crystal structures modeled in. The key feature is that the molecule bends at the junction between the lever arm and the rod, thus enabling the motor domains (magenta and red) to interact with the globular tail (yellow and orange). The site of interaction is near loop 1 at the entrance to the nucleotide-binding site (colored blue and green on the motor domain), providing a mechanism whereby activity is inhibited. The IQ motifs are colored the same as their respective motor domain, and CaM is in green. The observed length of the rod (cyan) is approximately equal to that between the lever arm and the PEST site. Figure adapted from [93].

Single particle analysis of negatively stained folded myoV molecules revealed a structure similar to that described above [86]. Approximately one-third of the total predicted coiled-coil region was clearly seen, the heads were in a post-power stroke conformation, and the site of interaction of the globular tail and the motor domain was far from the actin-binding site. A cluster of conserved acidic residues in the head, near

the entrance to the nucleotide binding site (between residues P117 and P137), was identified as a region that may interact with a basic cluster in the globular tail. An ionic interaction is consistent with the observation that high salt concentration (0.3 M NaCl) disrupts the folded conformation and causes myoV to adopt an extended conformation.

Only the ATPase of the full-length myoV construct is regulated, as shorter constructs do not contain all the structural elements necessary to form a folded conformation. Addition of the globular tail domain to truncated HMM constructs restores the inhibition of ATPase activity, and reconstitutes a triangular structure that resembles the folded full-length construct [85, 86]. Steady-state actin-activated ATPase assays show at most a tenfold difference in activity between the "on" and the "off" states of full-length myoV, which is not very tight regulation [26]. Based on studies of regulation of other myosin motors, it was realized that the inhibited rate can be strongly influenced by a few unregulated "rogue" molecules with high ATPase activity. Accordingly, single-turnover experiments, in which each motor domain is provided only one ATP molecule, is a better way to accurately assess the degree of regulation. By this technique, it was shown that the ATPase activity of the folded conformation (~0.2 s^{-1}) is at least 50-fold lower than the extended state (15 s^{-1}), a degree of regulation that should be effective *in vivo* [27].

Transition from the inhibited to active state

Near physiological salt concentration, calcium binding unfolds the molecule to the extended state, accompanied by an increase in actin-activated ATPase activity. The folded conformation shows no stabilizing interaction directly involving the lever arm, so how does calcium binding activate the molecule? Electron cryomicroscopy showed that calcium caused a major rearrangement of the bound CaMs in the lever arm [28], which could be sufficient to disrupt the motor domain-globular tail interaction and unfold the molecule.

An alternative pathway of activation is *via* cargo binding, given that cargo binding to the globular tail will presumably compete with its interaction with the motor domain. Although it makes biological sense that the motor should be activated only when needed for transport, it has not been directly demonstrated. Binding of melanophilin, the adapter protein for melanosomes, increased the actin-activated ATPase of myoV to approximately one-third the extent that calcium did. This activation was observed only at a salt concentration (0.2 M KCl) where the folded monomer was poised to unfold [87], implying that an additional factor is likely to be needed for full activation *via* this pathway.

Strategies for success in the cell

Cytoskeletal transport in mammalian cells involves interactions between processive molecular motors on both microtubule and actin tracks. In *Xenopus* melanocytes, pigment granules move toward the center of the cell in a process called aggregation, while they distribute more uniformly throughout the cell during dispersion, to cause skin color changes. This process requires switching between cytoskeletal tracks in both directions [88]. Microtubules are used for long-range, fairly linear transport from the nucleus to the cell periphery and back, while actin based transport is shorter and confined more to the cell periphery. The analogy that has been made is that microtubules are the highways in the cell, while actin tracks are the secondary roads.

Motors will need to navigate both microtubule-actin and actin-actin based intersections along the way. At the single molecule level, myoV effectively navigates actin-actin intersections either by executing a turn onto a crossing actin filament (~half of the time), by stepping over the crossing actin filament (~one-third of the time), or by terminating [89]. The frequency of turning *versus* stepping over can be accounted for simply by the number of actin-binding sites potentially available for the leading head to bind to in either situation. As described earlier, the unbound head searching for a new binding site undergoes a broad diffusional search in its quest to become the new leading head [16], and this is what occurs at an intersection. *In vivo*, however, cargo will likely contain multiple motors. In *Xenopus*, more than 60 myoV motors are estimated to be present on one melanosome, although only a few of these are expected to be engaged at one time [88]. The frequency of turning with multiple motors should differ from the single motor case, and will likely depend on the relative number of motors that are engaged with the original track *versus* the number that are sampling an intersecting track [90, 91].

How does cargo containing both kinesin and myoV execute a microtubule to actin transfer? One possibility is that the microtubule plus-end tracking protein EB1 is involved in the process [92]. The C-terminal region of melanophilin, the adapter protein that binds myoVa, contains a binding site for EB1. In principle this binding could allow melanophilin to "hitchhike" on EB1 to the end of the microtubule, at which point the tripartite protein transport complex consisting of

myoVa, melanophilin and the melanosome-bound Rab27a could be assembled for short-range transport on actin filaments. Another possible mechanism to facilitate cargo transfer between microtubules and actin is based on the observation that myoV can undergo a one-dimensional diffusional search on microtubules *in vitro*. In this non-energy-consuming process, myoV can scan long distances of the microtubule (>1.5 μm) for extended periods of time (>45 s), due to an electrostatic interaction between loop 2 in the myoV head, and a negatively charged region of tubulin called the E-hook [89]. In principle, this diffusive process could help myoV find cargo that is undergoing microtubule-based movement, and thus facilitate smooth transfer once a microtubule-actin intersection is encountered. The challenge that remains is to show whether either of these processes are operative in the cell, and to identify additional mechanisms that could facilitate cargo transport involving multiple tracks.

Remaining questions

Despite all that is known about myoV, many questions still remain. The full range of adapter proteins that link motor to cargo is still being discovered. How the functional transport complex is formed and then dissociated at the correct time and place is not fully understood, but progress has been made using the budding yeast system, where the key players can be readily manipulated genetically. It is still not clear if cargo-binding alone is sufficient to activate myoV from the folded conformation, and to what extent calcium regulates myoV function *in vivo*. The extent to which CaM *versus* a specific light chain, or the precise sequence of the IQ motifs itself, influences the ability of the lever arm to communicate strain to the motor domains is not known. Functional interactions between myoV and other motors in the cell, *via* their simultaneous presence on the same cargo, is an area of current investigation. Clearly the future still holds many challenges to fully understand the complex process of myoV-based cargo transport.

Acknowledgements. I thank Alex Hodges and Susan Lowey for helpful comments regarding the manuscript. This work was funded by NIH grant GM078097 to K.T.

1 Reck-Peterson, S. L., Provance, D. W. Jr., Mooseker, M. S. and Mercer, J. A. (2000) Class V myosins. Biochim. Biophys. Acta 1496, 36–51.
2 Rodriguez, O. C. and Cheney, R. E. (2002) Human myosin-Vc is a novel class V myosin expressed in epithelial cells. J. Cell Sci. 115, 991–1004.
3 Mercer, J. A., Seperack, P. K., Strobel, M. C., Copeland, N. G. and Jenkins, N. A. (1991) Novel myosin heavy chain encoded by murine dilute coat colour locus. Nature 349, 709–713.
4 Menasche, G., Ho, C. H., Sanal, O., Feldmann, J., Tezcan, I., Ersoy, F., Houdusse, A., Fischer, A. and de Saint Basile, G. (2003) Griscelli syndrome restricted to hypopigmentation results from a melanophilin defect (GS3) or a MYO5A F-exon deletion (GS1). J. Clin. Invest. 112, 450–456.
5 Roland, J. T., Kenworthy, A. K., Peranen, J., Caplan, S. and Goldenring, J. R. (2007) Myosin Vb interacts with Rab8a on a tubular network containing EHD1 and EHD3. Mol. Biol. Cell 18, 2828–2837.
6 Swiatecka-Urban, A., Talebian, L., Kanno, E., Moreau-Marquis, S., Coutermarsh, B., Hansen, K., Karlson, K. H., Barnaby, R., Cheney, R. E., Langford, G. M., Fukuda, M. and Stanton, B. A. (2007) Myosin Vb is required for trafficking of the cystic fibrosis transmembrane conductance regulator in Rab11a-specific apical recycling endosomes in polarized human airway epithelial cells. J. Biol. Chem. 282, 23725–23736.
7 Coureux, P. D., Wells, A. L., Menetrey, J., Yengo, C. M., Morris, C. A., Sweeney, H. L. and Houdusse, A. (2003) A structural state of the myosin V motor without bound nucleotide. Nature 425, 419–423.
8 Coureux, P. D., Sweeney, H. L. and Houdusse, A. (2004) Three myosin V structures delineate essential features of chemo-mechanical transduction. EMBO J. 23, 4527–4537.
9 Volkmann, N., Liu, H., Hazelwood, L., Krementsova, E. B., Lowey, S., Trybus, K. M. and Hanein, D. (2005) The structural basis of Myosin V processive movement as revealed by electron cryomicroscopy. Mol. Cell 19, 595–605.
10 Hodges, A. R., Krementsova, E. B. and Trybus, K. M. (2007) Engineering the processive run length of Myosin V. J. Biol. Chem. 282, 27192–27197.
11 Wang, F., Chen, L., Arcucci, O., Harvey, E. V., Bowers, B., Xu, Y., Hammer, J. A., 3rd and Sellers, J. R. (2000) Effect of ADP and ionic strength on the kinetic and motile properties of recombinant mouse myosin V. J. Biol. Chem. 275, 4329–4335.
12 Cheney, R. E., O'Shea, M. K., Heuser, J. E., Coelho, M. V., Wolenski, J. S., Espreafico, E. M., Forscher, P., Larson, R. E. and Mooseker, M. S. (1993) Brain myosin-V is a two-headed unconventional myosin with motor activity. Cell 75, 13–23.
13 Espindola, F. S., Suter, D. M., Partata, L. B., Cao, T., Wolenski, J. S., Cheney, R. E., King, S. M. and Mooseker, M. S. (2000) The light chain composition of chicken brain myosin-Va: Calmodulin, myosin-II essential light chains, and 8-kDa dynein light chain/PIN. Cell Motil. Cytoskeleton 47, 269–281.
14 Koide, H., Kinoshita, T., Tanaka, Y., Tanaka, S., Nagura, N., Meyer zu Horste, G., Miyagi, A. and Ando, T. (2006) Identification of the single specific IQ motif of myosin V from which calmodulin dissociates in the presence of Ca^{2+}. Biochemistry 45, 11598–11604.
15 De La Cruz, E. M., Wells, A. L., Sweeney, H. L. and Ostap, E. M. (2000) Actin and light chain isoform dependence of myosin V kinetics. Biochemistry 39, 14196–14202.
16 Dunn, A. R. and Spudich, J. A. (2007) Dynamics of the unbound head during myosin V processive translocation. Nat. Struct. Mol. Biol. 14, 246–248.
17 Terrak, M., Wu, G., Stafford, W. F., Lu, R. C. and Dominguez, R. (2003) Two distinct myosin light chain structures are induced by specific variations within the bound IQ motifs-functional implications. EMBO J. 22, 362–371.
18 Terrak, M., Rebowski, G., Lu, R. C., Grabarek, Z. and Dominguez, R. (2005) Structure of the light chain-binding domain of myosin V. Proc. Natl. Acad. Sci. USA 102, 12718–12723.
19 Walker, M. L., Burgess, S. A., Sellers, J. R., Wang, F., Hammer, J. A. 3rd, Trinick, J. and Knight, P. J. (2000) Two-headed binding of a processive myosin to F-actin. Nature 405, 804–807.
20 Ganoth, A., Nachliel, E., Friedman, R. and Gutman, M. (2007) Myosin V Movement: Lessons from molecular dynamics

studies of IQ peptides in the lever arm. Biochemistry 46, 14524–14536.
21 Pennestri, M., Melino, S., Contessa, G. M., Casavola, E. C., Paci, M., Ragnini-Wilson, A. and Cicero, D. O. (2007) Structural basis for the interaction of the myosin light chain Mlc1p with the myosin V Myo2p IQ motifs. J. Biol. Chem. 282, 667–679.
22 Watanabe, M., Nomura, K., Ohyama, A., Ishikawa, R., Komiya, Y., Hosaka, K., Yamauchi, E., Taniguchi, H., Sasakawa, N., Kumakura, K., Ushiki, T., Sato, O., Ikebe, M. and Igarashi, M. (2005) Myosin-Va regulates exocytosis through the submicromolar Ca^{2+}-dependent binding of syntaxin-1A. Mol. Biol. Cell 16, 4519–4530.
23 Kuboniwa, H., Tjandra, N., Grzesiek, S., Ren, H., Klee, C. B. and Bax, A. (1995) Solution structure of calcium-free calmodulin. Nat. Struct. Biol. 2, 768–776.
24 Zhang, M., Tanaka, T. and Ikura, M. (1995) Calcium-induced conformational transition revealed by the solution structure of apo calmodulin. Nat. Struct. Biol. 2, 758–767.
25 Houdusse, A., Gaucher, J. F., Krementsova, E., Mui, S., Trybus, K. M. and Cohen, C. (2006) Crystal structure of apocalmodulin bound to the first two IQ motifs of myosin V reveals essential recognition features. Proc. Natl. Acad. Sci. USA 103, 19326–19331.
26 Krementsov, D. N., Krementsova, E. B. and Trybus, K. M. (2004) Myosin V: Regulation by calcium, calmodulin, and the tail domain. J. Cell Biol. 164, 877–886.
27 Lu, H., Krementsova, E. B. and Trybus, K. M. (2006) Regulation of myosin V processivity by calcium at the single molecule level. J. Biol. Chem. 281, 31987–31994.
28 Trybus, K. M., Gushchin, M. I., Lui, H., Hazelwood, L., Krementsova, E. B., Volkmann, N. and Hanein, D. (2007) Effect of calcium on calmodulin bound to the IQ motifs of myosin V. J. Biol. Chem. 282, 23316–23325.
29 Moore, J. R., Krementsova, E. B., Trybus, K. M. and Warshaw, D. M. (2001) Myosin V exhibits a high duty cycle and large unitary displacement. J. Cell Biol. 155, 625–635.
30 Purcell, T. J., Morris, C., Spudich, J. A. and Sweeney, H. L. (2002) Role of the lever arm in the processive stepping of myosin V. Proc. Natl. Acad. Sci. USA 99, 14159–14164.
31 Sakamoto, T., Yildez, A., Selvin, P. R. and Sellers, J. R. (2005) Step-size is determined by neck length in myosin V. Biochemistry 44, 16203–16210.
32 Veigel, C., Wang, F., Bartoo, M. L., Sellers, J. R. and Molloy, J. E. (2002) The gated gait of the processive molecular motor, myosin V. Nat. Cell Biol. 4, 59–65.
33 Schott, D. H., Collins, R. N. and Bretscher, A. (2002) Secretory vesicle transport velocity in living cells depends on the myosin-V lever arm length. J. Cell Biol. 156, 35–39.
34 Wu, X., Bowers, B., Rao, K., Wei, Q. and Hammer, J. A. 3rd (1998) Visualization of melanosome dynamics within wild-type and dilute melanocytes suggests a paradigm for myosin V function *in vivo*. J. Cell Biol. 143, 1899–1918.
35 Wu, X., Rao, K., Bowers, M. B., Copeland, N. G., Jenkins, N. A. and Hammer, J. A. 3rd (2001) Rab27a enables myosin Va-dependent melanosome capture by recruiting the myosin to the organelle. J. Cell Sci. 114, 1091–1100.
36 Nascimento, A. A., Cheney, R. E., Tauhata, S. B., Larson, R. E. and Mooseker, M. S. (1996) Enzymatic characterization and functional domain mapping of brain myosin-V. J. Biol. Chem. 271, 17561–17569.
37 Seperack, P. K., Mercer, J. A., Strobel, M. C., Copeland, N. G. and Jenkins, N. A. (1995) Retroviral sequences located within an intron of the dilute gene alter dilute expression in a tissue-specific manner. EMBO J. 14, 2326–2332.
38 Wu, X. S., Rao, K., Zhang, H., Wang, F., Sellers, J. R., Matesic, L. E., Copeland, N. G., Jenkins, N. A. and Hammer, J. A. 3rd (2002) Identification of an organelle receptor for myosin-Va. Nat. Cell Biol. 4, 271–278.
39 Hodi, Z., Nemeth, A. L., Radnai, L., Hetenyi, C., Schlett, K., Bodor, A., Perczel, A. and Nyitray, L. (2006) Alternatively spliced exon B of myosin Va is essential for binding the tail-associated light chain shared by dynein. Biochemistry 45, 12582–12595.
40 Wagner, W., Fodor, E., Ginsburg, A. and Hammer, J. A. 3rd (2006) The binding of DYNLL2 to myosin Va requires alternatively spliced exon B and stabilizes a portion of the myosin's coiled-coil domain. Biochemistry 45, 11564–11577.
41 Puthalakath, H., Villunger, A., O'Reilly, L. A., Beaumont, J. G., Coultas, L., Cheney, R. E., Huang, D. C. and Strasser, A. (2001) Bmf: A proapoptotic BH3-only protein regulated by interaction with the myosin V actin motor complex, activated by anoikis. Science 293, 1829–1832.
42 Naisbitt, S., Valtschanoff, J., Allison, D. W., Sala, C., Kim, E., Craig, A. M., Weinberg, R. J. and Sheng, M. (2000) Interaction of the postsynaptic density-95/guanylate kinase domain-associated protein complex with a light chain of myosin-V and dynein. J. Neurosci. 20, 4524–4534.
43 Pashkova, N., Catlett, N. L., Novak, J. L., Wu, G., Lu, R., Cohen, R. E. and Weisman, L. S. (2005) Myosin V attachment to cargo requires the tight association of two functional subdomains. J. Cell Biol. 168, 359–364.
44 Catlett, N. L., Duex, J. E., Tang, F. and Weisman, L. S. (2000) Two distinct regions in a yeast myosin-V tail domain are required for the movement of different cargoes. J. Cell Biol. 150, 513–526.
45 Pashkova, N., Jin, Y., Ramaswamy, S. and Weisman, L. S. (2006) Structural basis for myosin V discrimination between distinct cargoes. EMBO J. 25, 693–700.
46 Huang, J. D., Cope, M. J., Mermall, V., Strobel, M. C., Kendrick-Jones, J., Russell, L. B., Mooseker, M. S., Copeland, N. G. and Jenkins, N. A. (1998) Molecular genetic dissection of mouse unconventional myosin-Va: Head region mutations. Genetics 148, 1951–1961.
47 Matesic, L. E., Yip, R., Reuss, A. E., Swing, D. A., O'Sullivan, T. N., Fletcher, C. F., Copeland, N. G. and Jenkins, N. A. (2001) Mutations in Mlph, encoding a member of the Rab effector family, cause the melanosome transport defects observed in leaden mice. Proc. Natl. Acad. Sci. USA 98, 10238–10243.
48 Wilson, S. M., Yip, R., Swing, D. A., O'Sullivan, T. N., Zhang, Y., Novak, E. K., Swank, R. T., Russell, L. B., Copeland, N. G. and Jenkins, N. A. (2000) A mutation in Rab27a causes the vesicle transport defects observed in ashen mice. Proc. Natl. Acad. Sci. USA 97, 7933–7938.
49 Fukuda, M., Kuroda, T. S. and Mikoshiba, K. (2002) Slac2-a/melanophilin, the missing link between Rab27 and myosin Va: Implications of a tripartite protein complex for melanosome transport. J. Biol. Chem. 277, 12432–12436.
50 Strom, M., Hume, A. N., Tarafder, A. K., Barkagianni, E. and Seabra, M. C. (2002) A family of Rab27-binding proteins. Melanophilin links Rab27a and myosin Va function in melanosome transport. J. Biol. Chem. 277, 25423–25430.
51 Geething, N. C. and Spudich, J. A. (2007) Identification of a minimal myosin Va binding site within an intrinsically unstructured domain of melanophilin. J. Biol. Chem. 282, 21518–21528.
52 Wu, X., Sakamoto, T., Zhang, F., Sellers, J. R. and Hammer, J. A. 3rd (2006) *In vitro* reconstitution of a transport complex containing Rab27a, melanophilin and myosin Va. FEBS Lett. 580, 5863–5868.
53 Hales, C. M., Vaerman, J. P. and Goldenring, J. R. (2002) Rab11 family interacting protein 2 associates with Myosin Vb and regulates plasma membrane recycling. J. Biol. Chem. 277, 50415–50421.
54 Lapierre, L. A., Kumar, R., Hales, C. M., Navarre, J., Bhartur, S. G., Burnette, J. O., Provance, D. W. Jr., Mercer, J. A., Bahler, M. and Goldenring, J. R. (2001) Myosin Vb is associated with plasma membrane recycling systems. Mol. Biol. Cell 12, 1843–1857.
55 Roland, J. T., Kenworthy, A. K., Peranen, J., Caplan, S. and Goldenring, J. R. (2007) Myosin Vb interacts with Rab8a on a tubular network containing EHD1 and EHD3. Mol. Biol. Cell 18, 2828–2837.

56 Gonsalvez, G. B., Urbinati, C. R. and Long, R. M. (2005) RNA localization in yeast: Moving towards a mechanism. Biol. Cell 97, 75–86.
57 Tang, F., Kauffman, E. J., Novak, J. L., Nau, J. J., Catlett, N. L. and Weisman, L. S. (2003) Regulated degradation of a class V myosin receptor directs movement of the yeast vacuole. Nature 422, 87–92.
58 Li, J. F. and Nebenfuhr, A. (2007) Organelle targeting of myosin XI is mediated by two globular tail subdomains with separate cargo binding sites. J. Biol. Chem. 282, 20593–20602.
59 Karcher, R. L., Roland, J. T., Zappacosta, F., Huddleston, M. J., Annan, R. S., Carr, S. A. and Gelfand, V. I. (2001) Cell cycle regulation of myosin-V by calcium/calmodulin-dependent protein kinase II. Science 293, 1317–1320.
60 Fukuda, M. and Itoh, T. (2004) Slac2-a/melanophilin contains multiple PEST-like sequences that are highly sensitive to proteolysis. J. Biol. Chem. 279, 22314–22321.
61 Mehta, A. D., Rock, R. S., Rief, M., Spudich, J. A., Mooseker, M. S. and Cheney, R. E. (1999) Myosin-V is a processive actin-based motor. Nature 400, 590–593.
62 Sellers, J. R. and Veigel, C. (2006) Walking with myosin V. Curr. Opin. Cell Biol. 18, 68–73.
63 De La Cruz, E. M., Wells, A. L., Rosenfeld, S. S., Ostap, E. M. and Sweeney, H. L. (1999) The kinetic mechanism of myosin V. Proc. Natl. Acad. Sci. USA 96, 13726–13731.
64 Baker, J. E., Krementsova, E. B., Kennedy, G. G., Armstrong, A., Trybus, K. M. and Warshaw, D. M. (2004) Myosin V processivity: Multiple kinetic pathways for head-to-head coordination. Proc. Natl. Acad. Sci. USA 101, 5542–5546.
65 Uemura, S., Higuchi, H., Olivares, A. O., De La Cruz, E. M. and Ishiwata, S. (2004) Mechanochemical coupling of two substeps in a single myosin V motor. Nat. Struct. Mol. Biol. 11, 877–883.
66 Yengo, C. M., De la Cruz, E. M., Safer, D., Ostap, E. M. and Sweeney, H. L. (2002) Kinetic characterization of the weak binding states of myosin V. Biochemistry 41, 8508–8517.
67 Yengo, C. M. and Sweeney, H. L. (2004) Functional role of loop 2 in myosin V. Biochemistry 43, 2605–2612.
68 Krementsova, E. B., Hodges, A. R., Lu, H. and Trybus, K. M. (2006) Processivity of chimeric class V myosins. J. Biol. Chem. 281, 6079–6086.
69 Rosenfeld, S. S. and Sweeney, H. L. (2004) A model of myosin V processivity. J. Biol. Chem. 279, 40100–40111.
70 Purcell, T. J., Sweeney, H. L. and Spudich, J. A. (2005) A force-dependent state controls the coordination of processive myosin V. Proc. Natl. Acad. Sci. USA 102, 13873–13878.
71 Veigel, C., Schmitz, S., Wang, F. and Sellers, J. R. (2005) Load-dependent kinetics of myosin-V can explain its high processivity. Nat. Cell Biol. 7, 861–869.
72 Forgacs, E., Cartwright, S., Sakamoto, T., Sellers, J. R., Corrie, J. E. T., Webb, M. R. and White, H. D. (2007) Kinetics of ADP dissociation from the trail and lead heads of actomyosin V following the power-stroke. J. Biol. Chem. 283, 766–773.
73 Yildiz, A., Forkey, J. N., McKinney, S. A., Ha, T., Goldman, Y. E. and Selvin, P. R. (2003) Myosin V walks hand-over-hand: Single fluorophore imaging with 1.5-nm localization. Science 300, 2061–2065.
74 Warshaw, D. M., Kennedy, G. G., Work, S. S., Krementsova, E. B., Beck, S. and Trybus, K. M. (2005) Differential labeling of myosin V heads with quantum dots allows direct visualization of hand-over-hand processivity. Biophys. J. 88, L30–32.
75 Shiroguchi, K. and Kinosita, K. Jr. (2007) Myosin V walks by lever action and Brownian motion. Science 316, 1208–1212.
76 Komori, Y., Iwane, A. H. and Yanagida, T. (2007) Myosin-V makes two brownian 90 degrees rotations per 36-nm step. Nat. Struct. Mol. Biol. 14, 968–973.
77 Levi, V., Gelfand, V. I., Serpinskaya, A. S. and Gratton, E. (2006) Melanosomes transported by myosin-V in Xenopus melanophores perform slow 35 nm steps. Biophys. J. 90, L07–09.
78 Kural, C., Serpinskaya, A. S., Chou, Y. H., Goldman, R. D., Gelfand, V. I. and Selvin, P. R. (2007) Tracking melanosomes inside a cell to study molecular motors and their interaction. Proc. Natl. Acad. Sci. USA 104, 5378–5382.
79 Li, X. D., Mabuchi, K., Ikebe, R. and Ikebe, M. (2004) Ca^{2+}-induced activation of ATPase activity of myosin Va is accompanied with a large conformational change. Biochem. Biophys. Res. Commun. 315, 538–545.
80 Wang, F., Thirumurugan, K., Stafford, W. F., Hammer, J. A. 3rd, Knight, P. J. and Sellers, J. R. (2004) Regulated conformation of myosin V. J. Biol. Chem. 279, 2333–2336.
81 Trybus, K. M., Huiatt, T. W. and Lowey, S. (1982) A bent monomeric conformation of myosin from smooth muscle. Proc. Natl. Acad. Sci. USA 79, 6151–6155.
82 Trybus, K. M. and Lowey, S. (1984) Conformational states of smooth muscle myosin. Effects of light chain phosphorylation and ionic strength. J. Biol. Chem. 259, 8564–8571.
83 Hackney, D. D., Levitt, J. D. and Suhan, J. (1992) Kinesin undergoes a 9 S to 6 S conformational transition. J. Biol. Chem. 267, 8696–8701.
84 Liu, J., Taylor, D. W., Krementsova, E. B., Trybus, K. M. and Taylor, K. A. (2006) Three-dimensional structure of the myosin V inhibited state by cryoelectron tomography. Nature 442, 208–211.
85 Li, X. D., Jung, H. S., Mabuchi, K., Craig, R. and Ikebe, M. (2006) The globular tail domain of myosin Va functions as an inhibitor of the myosin Va motor. J. Biol. Chem. 281, 21789–21798.
86 Thirumurugan, K., Sakamoto, T., Hammer, J. A. 3rd, Sellers, J. R. and Knight, P. J. (2006) The cargo-binding domain regulates structure and activity of myosin 5. Nature 442, 212–215.
87 Li, X. D., Ikebe, R. and Ikebe, M. (2005) Activation of myosin Va function by melanophilin, a specific docking partner of myosin Va. J. Biol. Chem. 280, 17815–17822.
88 Gross, S. P., Tuma, M. C., Deacon, S. W., Serpinskaya, A. S., Reilein, A. R. and Gelfand, V. I. (2002) Interactions and regulation of molecular motors in Xenopus melanophores. J. Cell Biol. 156, 855–865.
89 Ali, M. Y., Krementsova, E. B., Kennedy, G. G., Mahaffy, R., Pollard, T. D., Trybus, K. M. and Warshaw, D. M. (2007) Myosin Va maneuvers through actin intersections and diffuses along microtubules. Proc. Natl. Acad. Sci. USA 104, 4332–4336.
90 Snider, J., Lin, F., Zahedi, N., Rodionov, V., Yu, C. C. and Gross, S. P. (2004) Intracellular actin-based transport: How far you go depends on how often you switch. Proc. Natl. Acad. Sci. USA 101, 13204–13209.
91 Gross, S. P. (2007) Molecular motors: A tale of two filaments. Curr. Biol. 17, R277–280.
92 Wu, X. S., Tsan, G. L. and Hammer, J. A. 3rd (2005) Melanophilin and myosin Va track the microtubule plus end on EB1. J. Cell Biol. 171, 201–207.
93 Taylor, K. A. (2007) Regulation and recycling of myosin V. Curr. Opin. Cell Biol. 19, 67–74.